A comparison of vertical accuracy of global DEMs and DEMs produced by GEDI, ICESat-2

Narin, Omer Gokberk; Gullu, Mevlut

DOI
10.1007/s12145-023-01060-1

Publication date
2023

Document Version
Final published version

Published in
Earth Science Informatics

Citation (APA)
Narin, O. G., & Gullu, M. (2023). A comparison of vertical accuracy of global DEMs and DEMs produced by GEDI, ICESat-2. *Earth Science Informatics*, *16*(3), 2693-2707. https://doi.org/10.1007/s12145-023-01060-1

Earth Science Informatics
https://doi.org/10.1007/s12145-023-01060-1

RESEARCH

A comparison of vertical accuracy of global DEMs and DEMs produced by GEDI, ICESat-2

Omer Gokberk Narin[1,2] · Mevlut Gullu[1]

Received: 24 April 2023 / Accepted: 21 July 2023

Abstract
Digital elevation models (DEM) are an essential data source in many professional disciplines, with the help of gridded height information and values such as slope and aspect produced from that information. In this study, Ice, Cloud and land Elevation Satellite-2 (ICESat-2) and Global Ecosystem Dynamics Investigation (GEDI) satellite-altimetry data, and SRTM, ASTER-GDEM, and ALOS World3D data were used as Global DEMs (GDEMs) data in three different areas (U.S.A., New Zealand and Puerto Rico). We used kriging methods for interpolation to create the new rasters. Point-based accuracies were compared with the GDEMs from satellite-altimetry systems and raster-based comparisons were made by deriving DEMs with satellite-altimetry data in three different areas. It was seen that the ICESat-2 data in point-based results had similar accuracy with other GDEMs. DEMs produced by using ICESat-2 and GEDI data together gave relatively better results than using alone. In particular, the correlation was found to be highly correlated with 99%.

Keywords ICESat-2 · GEDI · Satellite-Based LiDAR · Global Digital Elevation Models (GDEMs)

Introduction

Digital Elevation Models (DEMs) are important data sources in many professional disciplines, especially earth sciences applications. This data can be produced in different scales and with various methods for different purposes. These are Global Navigation Satellite System-Precise Point Positioning (GNSS-PPP) (Abdallah et al. 2020), levelling (Erdogan 2009), Unmanned Aerial Vehicle (UAV), photogrammetry (Uysal et al. 2015), and aerial or terrestrial Laser Imaging Detection and Ranging (LiDAR) (Liu et al. 2008; Heritage et al. 2009), passive stereo (ASTER, ALOS) and active (SRTM, TanDEM X) remote sensing, but in our study, we wanted to test whether Satellite Altimetry Systems (SAS) (Global Ecosystem Dynamics Investigation (GEDI), ICESat-2) systems would be successful in DEM production. DEMs contain different information and they have been used to extract various features. These can be geographical features of the region (mountain, hill, valley, plain, etc.) and terrain information (slope, aspect, etc.). In addition to this, DEMs can be used as an input data for different applications such as mapping of soil type distribution (Park et al. 2001), mountain glacier change (Jaber et al. 2013), river change estimation (Milan et al. 2011), bathymetry (Muslim and Foody 2008), water flow modeling (Petrasova et al. 2017), forest canopy calculation (Kassim et al. 2016), etc.

DEM production methods mentioned above have advantages and disadvantages over each other. The production of DEMs varies according to spatial resolution, data accuracy, and the size of the study area. For this reason, it is essential both in terms of time and cost to determine the purpose and method of DEMs production according to the usage area. There are also global DEM data produced to be used as a base in many studies. These data are mosaic data covering a particular period or year, such as SRTM, Aster GDEM and ALOS World 3D-30 m (AW3D30). The accuracy analysis of these data was performed by comparing them with measurements such as local GPS (El Mhamdi et al. 2023; Preety et al. 2022), Airbone Laser Scanning (ALS) and leveling in different studies (Mesa-Mingorance and Ariza-López 2020). Santillan and Makinano-Santillan (2016) compared the data of SRTM, Aster GDEM and ALOS World 3D-30 m (AW3D30) in their study. They chose the Northeastern Mindanao region

Communicated by: H. Babaie

✉ Omer Gokberk Narin
gokberknarin@aku.edu.tr

1 Geomatics Engineering Department, Afyon Kocatepe University, 03100 Afyonkarahisar, Turkey

2 Department of Geoscience and Remote Sensing, Delft University of Technology, PO Box 5048, 2600GA Delft, the Netherlands

of the Philippines as the comparison area. As a result of the study, with RMSE = 5.68 m. the AW3D30 data gives the best results. Yap et al. (2019) used SRTM, Aster GDEM, and AW3D30 data in their study to examine the whole of Cameroon. As a result of the study, they stated that the AW3D30 data gave the best results. Deveraj and Yarrakula (2020), 1/50000 scaled survey of India maps, which are presented as open data of India as a reference, were used, and calculated on 269 samples. SRTM-30, SRTM-90, ASTER, SENTINEL-1, TANDEM, ALOS PALSAR DEM and CartoDEM were used as comparison data. The mountainous area in the Western Ghats of India was chosen as the study area. As a result, it was stated that the SRTM-30 height data was better, and they also stated that more tests should be done since DEMs are one of the main inputs in various applications. Wong et al. (2014) compared LiDAR data with SRTM and ASTER GDEM v2 data. They selected 2 study areas and obtained accuracies Standard Deviation (SD) = 9.0 m-10.4 m; RMSE = 9.3 m-10.6 m for SRTM, (SD = 16.9 m-18.7 m; RMSE = 17.0 m-19.3 m) for ASTER GDEM.

In 2018, compared to above mentioned missions relatively new two SAS, whose purpose is to monitor 3-D structures on Earth, began to collect data. While the first purpose of Global Ecosystems Dynamic Investigation (GEDI) among these systems was to monitor forests, the first purpose of Ice, Cloud, and land Elevation Satellite-2 (ICESat-2) was to monitor glaciers. However, both systems help to collect 3-D data for use in the world for different purposes. GEDI Laser altimetry was placed on the International Space Station (ISS) in December 2018 and began collecting data between 51.6° North and 51.6° South latitude (Dubayah et al. 2020). Although the priority of the GEDI task is the vertical structure of the forest, with the help of the data obtained, topography, water body altimeter, archaeological, etc., can be used in studies. Fayad et al. (2020) investigated the lake water levels with GEDI. Their research stated that there were various systematic errors in different periods. As a result of the study, they concluded that there were -26.8 and + 15.2 cm errors between GEDI and hydrological gauges data. Kokalj and Mast (2021) investigated detection of archaeological remains in a forested area with GEDI data. They determined one of the Maya cities in the Yucatan peninsula as the study area. As a result of the study, they stated that due to the low scanning density of GEDI points, they are not suitable for archeology studies yet.

Quirós et al. (2021) compared DEMs with 12,031 GEDI footprints in 10 different regions in Spain. The Root Mean Square Error (RMSE) of the comparison of GEDI and LiDAR data was 6.13 m. They stated that they reached RMSE values much lower than this value in some regions. In addition, they reported that when the positional errors of GEDI points are eliminated, they give better results. Adam et al. (2020) studied two different areas in Germany, they examined both terrain and canopy data with 69,927 GEDI points. They used the Median Absolute Deviation (MAD) criterion in the study. They found the error of 2.55 m and 3.10 m for the terrain, 0.97 m, and 0.30 m for the canopy. They also reported 9–13% outliers, which reduces the precision of the estimation. Liu et al. (2021) compared ICESat-2 and GEDI data in 40 different fields. Since 5 of these areas are in Alaska, only ICESat-2 data was examined. The other 35 areas were evaluated, 90,472 GEDI and 32,666 ICESat-2 points for the terrain. As a result, they found RMSE = 4.03 m for GEDI and RMSE = 2.24 m for ICESat-2 at the surface at mid and low latitudes. In addition, as a result of the study, they stated that even though the two products have different properties, they can advantage from their use together. Neuenschwander and Magruder (2019) conducted their first study on ICESat-2 in a vegetated area of Finland. They used a single section in the study and 854 points for the canopy and 1,105 for the surface. As a result of the study, they found an error of 5 m horizontally and RMSE = 0.85 m, R^2 = 0.99 for terrain, RMSE = 3.69, and R^2 = 0.982 for the canopy in the vertical direction.

Shang et al. (2022), aimed to obtain control points for ICESat-2 data in two different fields. In this context, they have determined a 9-step filtering strategy and as a result, the accuracy of ICESat-2 data is reduced to RMSE = 0.5 m.

In our study, besides point-based comparison, we created a DEM from ICESat-2 and GEDI data and made a raster-based comparison. There are different interpolation methods in DEM generation such as Inverse distance weighting (IDW), Ordinary Kriging (ORK), Simple Kriging (SIK), Radial Basis Functions (RBF), Global Polynomial Interpolation (GPI), Local Polynomial Interpolation (LPI) and Fuzzy Logic etc. Banjo et al. (2021), compared IDW, ORK, SIK, Empirical Bayesian Kriging (EBK), GPI, LPI and Kernel Interpolation with Barrier (KIB) methods and stated that the ORK method gave the best results (RMSE = 7.794 m). Setiyoko and Kumar (2012) used deterministic (IDW, GPI, LPI, and RBF) and probabilistic (SIK, ORK, universal kriging, indicator kriging, probabilistic kriging, disjunctive kriging, and cokriging) interpolation methods. As a result of the study, they stated that the ORK interpolation method gave the least error (avg. error = 1.29 m). Sunila and Kollo (2007) compared the kriging method with the fuzzy logic method in their study. They stated that the ORK method gave better results (RMSE = 3.27 m).

In this study, we investigated i) To generalize the quality of the GEDI and ICESat data three study areas from different countries were evaluated. ii) to compare GEDI and ICESat-2 data with GDEMs on a point-based analysis (Sect. 3.1). iii) to produce DEM from GEDI, ICESat-2, and a combination of GEDI and ICESat-2, which is not investigated before in the literature. The generated DEMs and GDEMs were compared with the raster-based ALS DEM data.

Material and methods

Study area

While choosing the study area, three different areas with different locations (Fig. 1) heights and slopes were selected (Table 1). The first of these areas were selected from the Washington state classes north of the U.S.A. This study area will be referred to as test area-1 in other parts of the article. The second of the fields was selected from the island of Puerto Rico. This study area will be referred to as test area-2 in other parts of the article. The third of the areas, the Bank Peninsula, located on the east coast New Zealand's South Island, was chosen. This study area will be referred to as test area-3 in the next sections of the article. Test area-1 and Test area-3 are mountainous areas, while in test area-2 southern parts are mountainous and northern parts are flat areas. In addition, test area-1 and test area-2 are densely covered with forested areas, while test area-3 generally consists of bare lands. Other information about the fields is given in Table 1.

Ground truth

In the study, we used DEM generated from ALS as ground truth. ALS data is also downloaded in raster format. There are

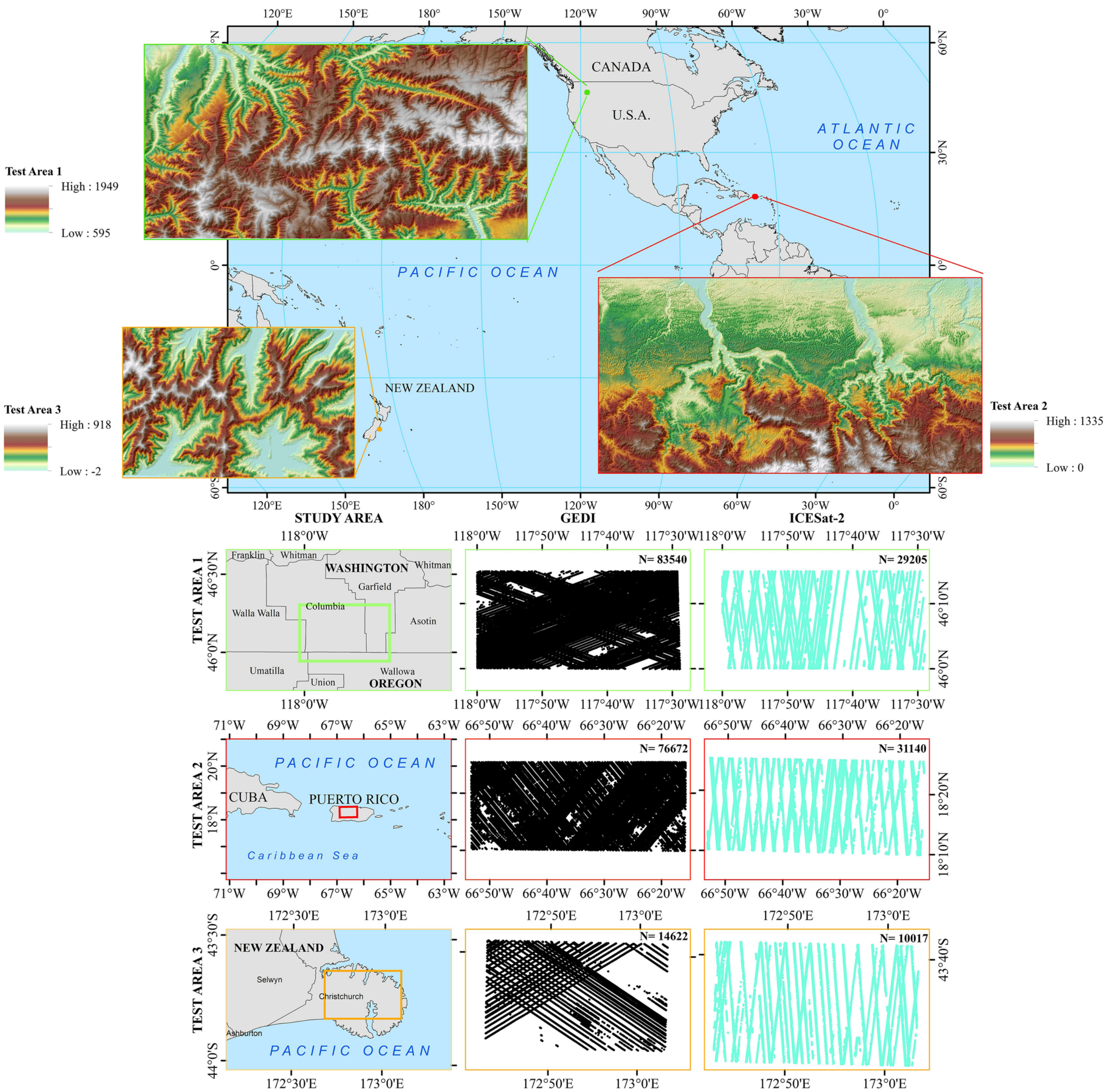

Fig. 1 Study areas. The height values are in meter

Table 1 Information of Study Areas

	Test Area 1	Test Area 2	Test Area 3
Country Name	U.S.A	Puerto Rico	New Zealand
Central Coordinates (WGS 1984)	46° 7′31.82"N 117°44′37.12"W	18°16′46.54"N 66°34′26.98"W	43°43′12.69"S 172°53′25.06"E
Area (km^2)	~1100	~2.037	~400
Min. – Max. Height (m)	594.67–1948.59	0 – 1335.46	-2 – 918
Average Height (m)	1326.51	380.99	302.78
Min. – Max. Slope (%)	0 – 53.99	0 –72.96	0 – 62.52
Average Slope (%)	23.55	17.93	19.26
Source	https://lidarportal.dnr.wa.gov/	https://www.sciencebase.gov/catalog/item/5eb7a41882ce25b5135d09c1	https://doi.org/10.5069/G98W3BHC

differences in ALS scanners because the study is in more than one region, and there are data produced by different countries or programs. But the data's acquisition date and vertical accuracy are close to each other. DEM data obtained from ALS are used as accepted reference data for accuracy analysis in different studies in the literature. (Adam et al. 2020; Liu et al. 2021). Ground truth data are all orthometric height (H). The technical information about the data is given in Table 2.

Satellite altimetry systems

Data collection from the GEDI and ICESat-2 satellites has become an essential source for space-based altimetry systems. In addition, similar coverage areas and data collected on the same dates both increase the point density in the area and are essential in comparing the two systems. Although both systems are space-based, there are differences between them. In the study, the height values were reduced to the EGM96 (Lemoine et al. 1998) geoid to match the GDEMs and the vertical datum. The geoid heights were obtained from The International Center for Global Earth Models (ICGEM). ICGEM is a system that has offered Global Gravity field data and many other data free of charge since 2003 (Ince et al. 2019). A user-defined point module was used in ICGEM to calculate the geoid height (N) value for points GEDI and ICESat-2 (http://icgem.gfz-potsdam.de/calcpoints).

GEDI

GEDI collects data between latitudes 51.6° N and 51.6° S. GEDI is a full wavelength LiDAR system that sends a laser beam at a wavelength of 1064 nm (near IR). As the GEDI laser system is integrated into the International Space Station, its temporal resolution and revisit period vary. In addition, GEDI collected data for two years (2019–2020). The spatial resolution is approximately 30 m in diameter. GEDI's latitude, longitude, and altitude information are geographic coordinates in the WGS 84 system (Dubayah et al. 2020). In the study, all data of GEDI for two years were evaluated. Within the scope of the study, we downloaded GEDI level 2A data. Data with quality flag "1" were selected (The elevation of center of the lowest mode of the received waveform in the footprint relative to the reference ellipsoid (elev_lowestmode)) from Level 2A products and evaluated without preprocessing or filtering in the study (Table 3).

ICESat-2

ICESat-2 collects data between latitudes 88° N and 88° S. The ICESat-2 uses a photon-counting LiDAR system and emits a beam at a wavelength of 532 nm (green). ICESat-2 has a temporal resolution of approximately three months. The latitude, longitude, and altitude information produced in ICESat-2 are geographic coordinates in the WGS 84 system (Neuenschwander and Magruder 2019). Within the scope of the study, we downloaded the ICESat-2 ATL08 version (Neuenschwander et al. 2020). Best elevation for surface in the footprint relative to the Reference Ellipsoid (h_te_best_fit) from ATL08 level are used. ICESat-2 data was downloaded from the openaltimetry site (Khalsa et al. 2020). All ICESat-2 data published up to 1 January 2022 were used (Table 3).

Table 2 Technical Information of ALS used for comparison

	Test Area 1	Test Area 2	Test Area 3
Acquisition Date	2018	2018	2018–2019
Flight Height (m)	1650–2100 AGL	700–1000 AGL	1525–2200 AGL
Point Density (pts/m^2)	8	42	6
Vertical Accuracy (RMSE)	0.10 m	0.13 m	0.028 m
Source	https://lidarportal.dnr.wa.gov/	https://www.sciencebase.gov/catalog/item/5eb7a41882ce25b5135d09c1	https://doi.org/10.5069/G98W3BHC

Table 3 Technical Information of GEDI and ICESat-2

Mission	ICESat-2	GEDI
Projection	Geographic	Geographic
Horizontal Datum	WGS84	WGS84
Vertical Datum	WGS84	WGS84
Launch Date	September, 2018	December, 2018
Coverage Area	88° N – 88° S Latitude	51.6° N –51.6° S Latitude
Sensor Wavelength	532 nm (green)	1064 nm (near IR)
Organization	NASA	NASA
Source	https://icesat-2.gsfc.nasa.gov/	https://gedi.umd.edu/

We examined the number of points per km^2 of GEDI and ICESat-2 data (Table 4). GEDI is integrated with the ISS and has a high revisit time, it has collected more points in almost the same period, but the temporal resolution of ICESat-2 is 3 months. Looking at Table 4, it was determined that the highest usable point density was in test area 1.

Global Digital Elevation Systems

ALOS WORLD 3D

The Advanced Land Observing Satellite (ALOS) was developed by JAXA in 2006. The ALOS satellite is built to collect global data and is equipped with a Panchromatic Remote-sensing Instrument for Stereo Mapping (PRISM) sensor. ALOS collected data between 2006 and 2011. JAXA first released AW3D30 in 2015 (Version 1.0). Many improvements have been made since then. The AW3D30 footprint is between 60° N and 60° S latitudes (https://www.eorc.jaxa.jp/ALOS/en/aw3d30/aw3d30v3.2_product_e_e1.2.pdf). Other information about the AW3D30 is given in Table 5. Our study, was used version 3.2.

Table 4 The number of GEDI and ICESat-2 points per Km^2 for each test area

	Area (Km^2)	Point		Point Density (Km^2/point)	
		GEDI	ICESat-2	GEDI	ICESat-2
Test Area 1	1093	83,540	29,205	76.43	26.72
Test Area 2	2037	76,672	31,140	37.64	15.29
Test Area 3	462	14,622	10,017	31.65	21.68

ASTER GDEM

ASTER is an optical sensor satellite jointly developed by NASA and METI. ASTER GDEM is a GDEM created with images collected from the ASTER satellite. Version 1 was announced in 2009 and manufactured at Data Sensor Information Laboratory Corporation (SILC) Tokyo. Many improvements have been made since then. The footprint of ASTER GDEM is between latitudes 83° N and 83° S (https://lpdaac.usgs.gov/documents/434/ASTGTM_User_Guide_V3.pdf). Other information about ASTER GDEM is given in Table 5. Our study, was used version 3 (ASTER GDEM V3).

SRTM

SRTM is a project by NASA for the creation of GDEM. During its 11-day mission on February 11, 2000, Synthetic Aperture Radar (SAR) images were collected between latitudes 60° N—60° S. SRTM published the first version in 2003. Many improvements have been made since then. Other information about SRTM is given in Table 5. In our study, a version 3 was used.

Kriging interpolation method and DEM production

In our study, we used the kriging interpolation method to generate DEM with GEDI and ICESat-2 data. Kriging is an

Table 5 Technical Information of GDEMs

GDEMs	ALOS WORLD 3D	ASTER GDEM	SRTM
Projection	Geographic	Geographic	Geographic
Horizontal Datum	GRS80 (ITRF97)	WGS84	WGS84
Vertical Datum	EGM96	EGM96	EGM96
Acquisition Date	2006–2011	2000–2013	2000
Sensor	Optical	Optical	Radar (C band)
Resolution (m)	~30	~30	~30
Organization	JAXA	NASA/METI	NASA
Source	https://www.eorc.jaxa.jp/ALOS/en/aw3d30/aw3d30v3.2_product_e_e1.2.pdf	https://lpdaac.usgs.gov/documents/434/ASTGTM_User_Guide_V3.pdf	https://lpdaac.usgs.gov/documents/179/SRTM_User_Guide_V3.pdf

interpolation method that uses a variogram based on the spatial distribution of known points' positions (Burrough 1986; Oliver and Webster 1990). DEMs were produced in 1 arc-second spatial resolution. In the study, 3 different DEMs were produced for each area. Firstly, only with GEDI points, secondly only with ICESat-2 points and thirdly a combination of GEDI and ICESat-2 points was used for DEM generation.

Methodology & accuracy assessment

Open-source ALS data was used as validation data to test GEDI and ICESat-2 data at different latitudes and longitudes, slopes, elevations, and hemispheres. Three test areas showing these differences were examined. ALS data were selected from data collected in 2018 to avoid temporal differences between study areas and SAS data. In this context, we analyzed all the published data of GEDI (Level-2a) products until the end of 2020 and ICESat-2 (ATL-08) products until the end of 2021. We compared GEDI and ICESat-2's footprint data with ALOS World 3D, ASTER, and SRTM on a point-based. For comparison, elevation data of the projections of both GEDI and ICESat-2 points were obtained separately in each test area. The accuracy of the ICESat-2 and GDEMs data and the accuracy of the GEDI and GDEMS data were then examined separately. Then, DEM was created for each area by the combination of GEDI and ICESat-2 data together. The ORK method was used while creating DEMs. The created DEMs were produced at the same resolution as the GDEM. Error distribution graphs of the data were created and interpreted according to the ground truth data. We evaluated the results using Mean Absolute Error (MAE), R.^{2}, RMSE, MAD (Urbazaev et al. 2022) calculated from Eq. 1, Eq. 2, Eq. 3 and Eq. 4 given below. Besides, the workflow of the methodology is given in Fig. 2. The statistical analysis and visualization were done using the statistical software R 4.1.0 (Team RC 2013).

$$MAE = \frac{1}{n}\sum_{i=1}^{n}\left|x_i^a - x_i^b\right| \tag{1}$$

$$R^2 = \frac{\sum\left(x_i^a - \overline{x_i^a}\right)\left(x_i^b - \overline{x_i^b}\right)}{\sqrt{\sum\left(x_i^a - \overline{x_i^a}\right)^2\left(x_i^b - \overline{x_i^b}\right)^2}} \tag{2}$$

$$RMSE = \sqrt{\frac{1}{n}\sum_{i=1}^{n}\left(x_i^a - x_i^b\right)^2} \tag{3}$$

$$MAD = median\left(\left|\ \left(x_i^a - x_i^b\right) - median\left(x_i^a - x_i^b\right)\ \right|\right) \tag{4}$$

where n is the number of GEDI or ICESat-2, and random point data, x_i^a is the ALS data vertical value, and x_i^b is the GEDI, ICESat-2, produced DEM, and GDEM data vertical values, $\overline{x_i^a}$ is ALS data average vertical value, $\overline{x_i^b}$ is the GEDI, ICESat-2, produced DEM, and GDEMs data average vertical values.

Results

Point-based results

The spatial error distribution of GEDI and ICESat-2 points is given in Fig. 3. While giving the spatial error distributions, the points with vertical errors between -20 m and + 20 m are not shown.

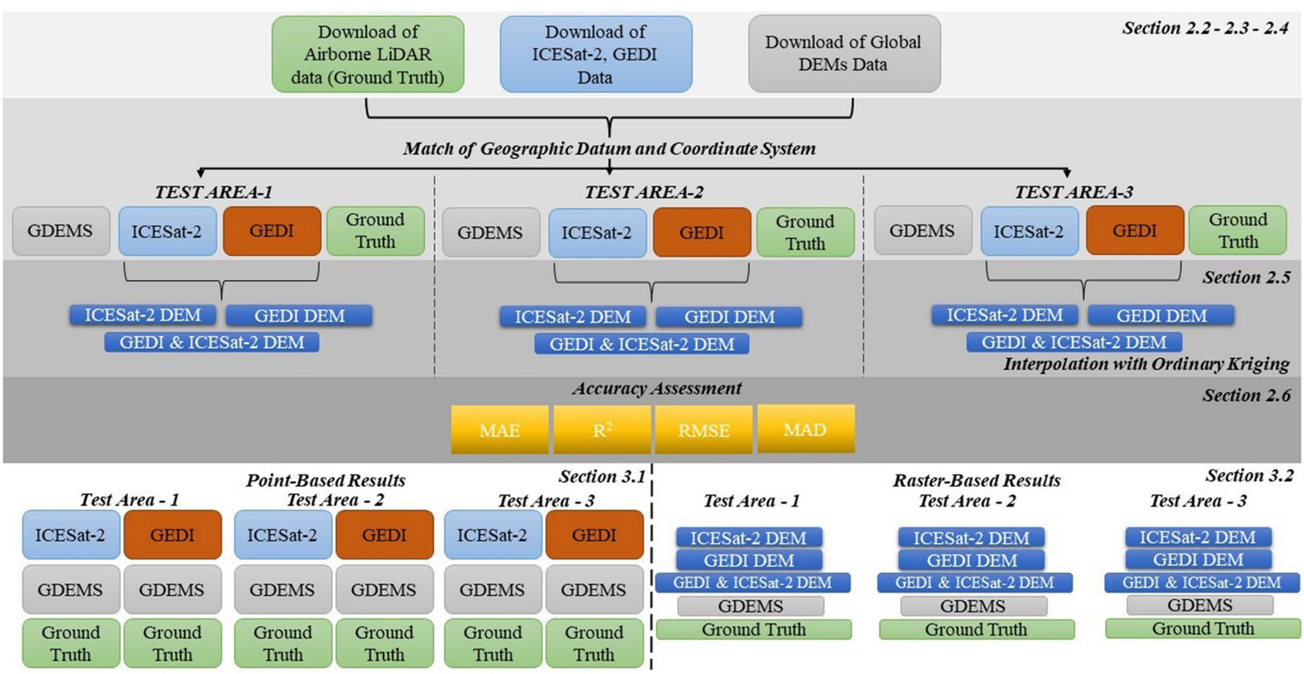

Fig. 2 The workflow of the methodology

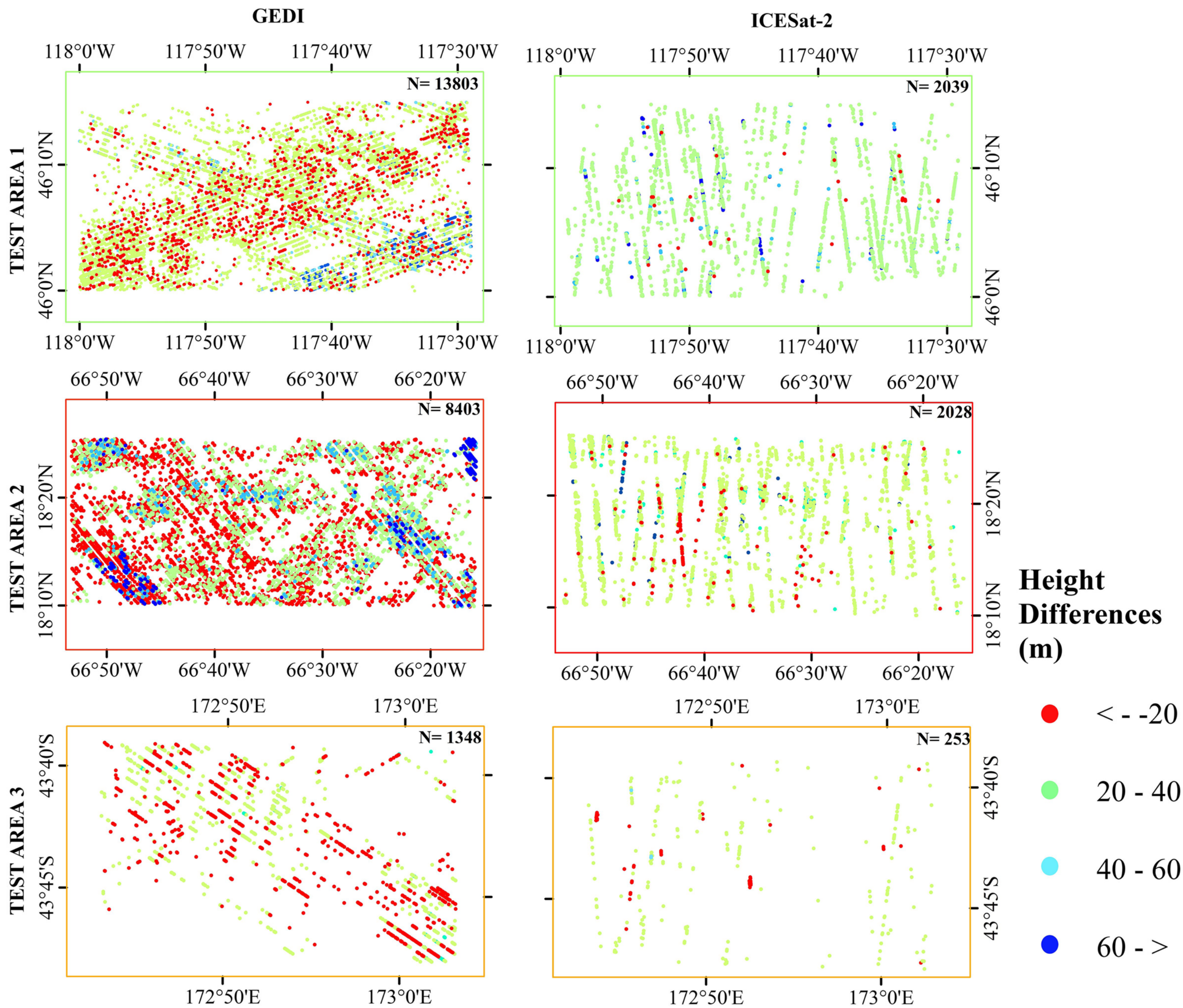

Fig. 3 Spatial distribution of height differences of points GEDI and ICESat-2 compared to ALS for each test area

ICESat-2 data shows that there is more than 93% data distribution in the range of -20 –+20 in all 3 test areas (Table 6). In GEDI data, on the other hand, this rate varies and it is seen that there is a data distribution between 83 and 90% (Table 6). GEDI, ICESat-2 and GDEMs were compared with ALS data at each Test Area (Fig. 4). Although Test Area-1 (22.350 m) and Test Area-2 (20.359 m) gave the worst results in Point-based comparison results according to RMSE of GEDI's footprint, Test Area-3 (11.952 m) also gave better results than ASTER GDEM. In addition, AW3D30 gave the best results for Test Area-1 (12.292 m) and Test Area-2 (13.578 m) among GDEMs, while SRTM gave the best results for Test Area-3 (6.623 m). According to the RMSE point-based comparison results of ICESat-2's footprints, Test area-1 (12.166 m) also gave the best result after AW3D30, In Test Area-2, ASTER GDEM (17.044 m) gave the worst result, while the other 3 data gave similar results with 13 m RMSE. In Test Area-3, ICESat-2 (7.846 m) gave the best result after SRTM (6.172 m) (Appendix Table 7). According to MAD results, GEDI gave the best results between 0.226 m and 3,530 m in all areas, while ICESat-2 gave the best results in all areas except Test Area-2. When we compared the areas according to RMSE, test area-3 gave the best results. (Fig. 5).

Raster-based results

The ORK method was used in the production of DEM (Fig. 6). Difference maps and histograms were produced for each test area of the ground truth differences with GDEMs and generated DEMs (Figs. 7, 8, 9, 10, 11 and 12). In addition, a comparative chart including RMSE, MAE, MAD results was created for all test areas (Fig. 13). The accuracies of the produced DEMs have been tested on a raster-based assessment. Due to the gaps in the ICESat-2 data for test area-1(Fig. 7), DEM production

Table 6 GEDI and ICESat-2 error distribution rates

	GEDI			ICESat-2		
	Range (m)	Beams	Ratio %	Range (m)	Beams	Ratio %
Test Area 1	<— -20	5253	6.288	<— -20	38	0.130
	-20 — 20	69,737	83.477	-20 — 20	27,166	93.018
	20 — 40	6386	7.644	20 — 40	1734	5.937
	40 — 60	1105	1.323	40 — 60	160	0.548
	60 —>	1059	1.268	60 —>	107	0.366
Test Area 2	<— -20	4702	6.133	<— -20	128	0.411
	-20 — 20	68,269	89.040	-20 — 20	29,112	93.487
	20 — 40	2816	3.673	20 — 40	1646	5.286
	40 — 60	468	0.610	40 — 60	181	0.581
	60 —>	417	0.544	60 —>	73	0.234
Test Area 3	<— -20	673	4.603	<— -20	45	0.449
	-20 — 20	13,274	90.781	-20 — 20	9764	97.474
	20 — 40	598	4.090	20 — 40	205	2.047
	40 — 60	70	0.479	40 — 60	3	0.030
	60 —>	7	0.048	60 —>	0	0.000

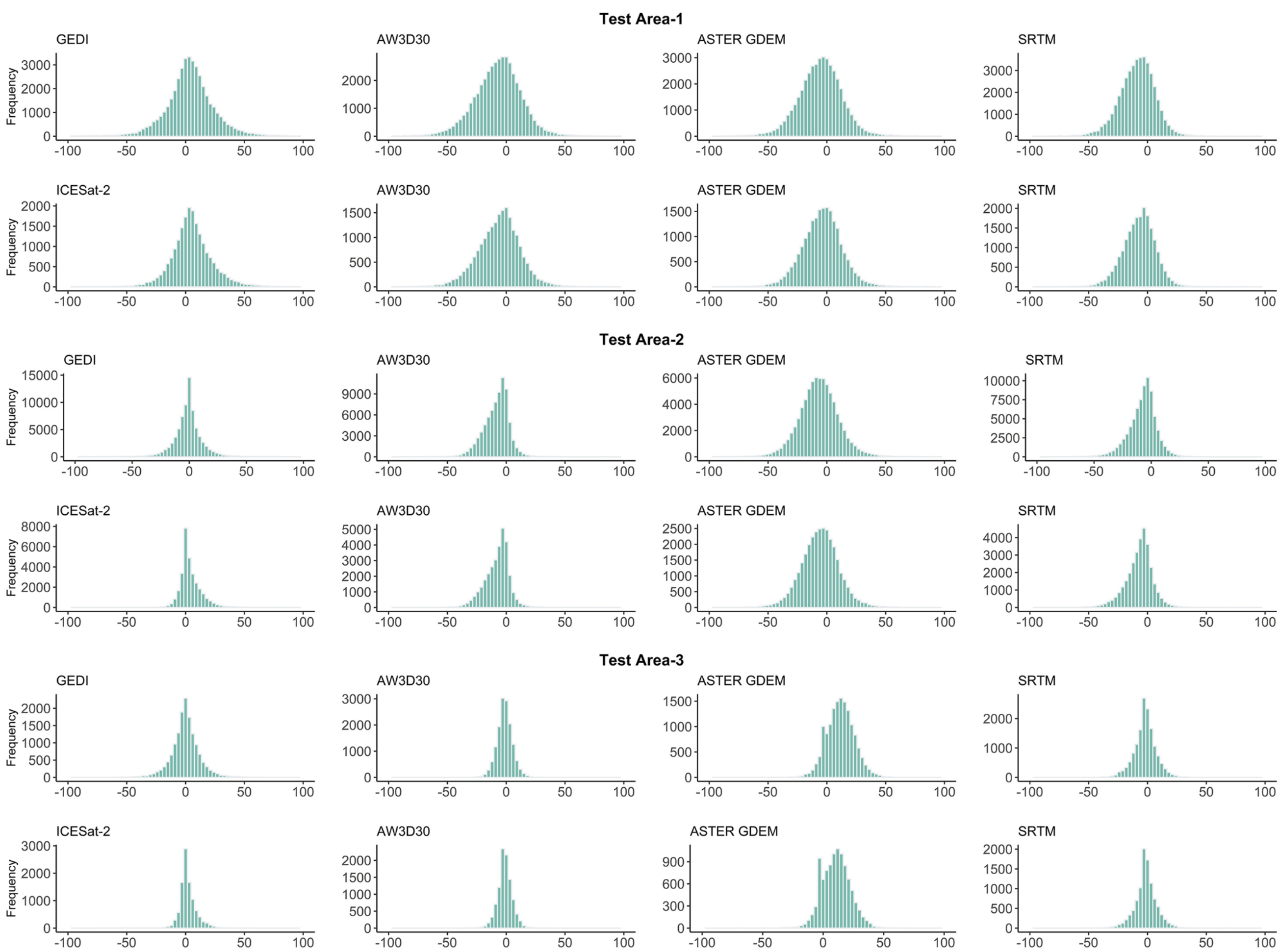

Fig. 4 Point based error histogram graphics

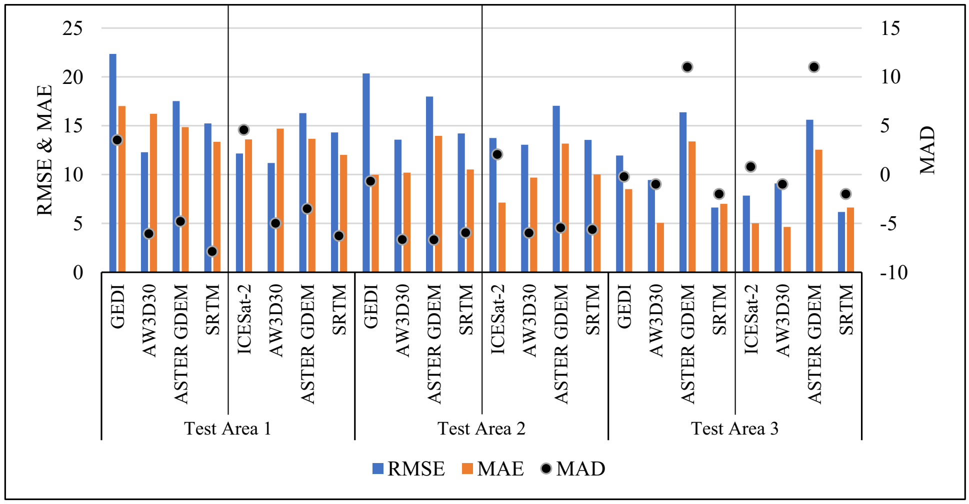

Fig. 5 Point-based assessment based on ALS data

gave worse results than GEDI according to RMSE (Appendix Table 7). Looking at the results for DEM, ICESat-2 gave the worst result, with a RMSE value of 51.788 m. Although the error decreased by 23.692 m when GEDI and ICESat-2 were combined, it could not approach the sensitivity of other GDEMs. The AW3D30 showed the best results for test area-1 with 13.538 m (Fig. 13). When the results are analyzed according to MAD in test area-1, it is seen that the DEM produced with GEDI gives the best result with 2.857 m. (Fig. 13). Test area-2 gave better results than test area-1 (Fig. 8). However, it has 10–15 m more errors than other GDEMs (Fig. 10). The AW3D30 also gave the best results in test area-2 (Fig. 13). When the results are examined according to MAD in test area-2, it is seen that the DEM produced with GEDI & ICESat-2 gives the best result with 0.166 m. (Fig. 13). Test area-3 has more gaps in the GEDI data than other areas (Fig. 1). Due to these gaps, GEDI data gave the worst RMSE result here at 91.217 m. When the two data are combined, although it gives results according to 39.954 m RMSE, it is quite unsuccessful compared to other GDEMs. In test area-3, the SRTM gave the best results with 6.434 m (Fig. 12). When the results are analyzed according to MAD in test area-3, it is obtained that the DEM produced with the combination of GEDI and ICESat-2 gives the best results at 0.843 m (Fig. 13). When looking at the raster-based results in general, although the results are low according to RMSE, good results are obtained according to the MAD.

Discussion

Considering satellite lidar systems, the previous studies analyzed a point-based comparison. Many studies in the literature stated that GEDI and ICESat-2 data gave better results after filtering the data due to various reasons (day & night, spatial errors, cloudiness, terrain structure, etc.). (Quirós et al. 2021; Adam et al. 2020; Liu et al. 2021). Adam et al. (2020) stated in their study that 9–13% of the GEDI data were outliers. In our study, the results of GEDI the outliers ranges between 11 and 16%, while ICESat-2 has lower as 3% to 7% outliers. Shang et al. (2022) reached up to 0.5 m. accuracy after filtering ICESat-2 data. However, it is seen that the number of points

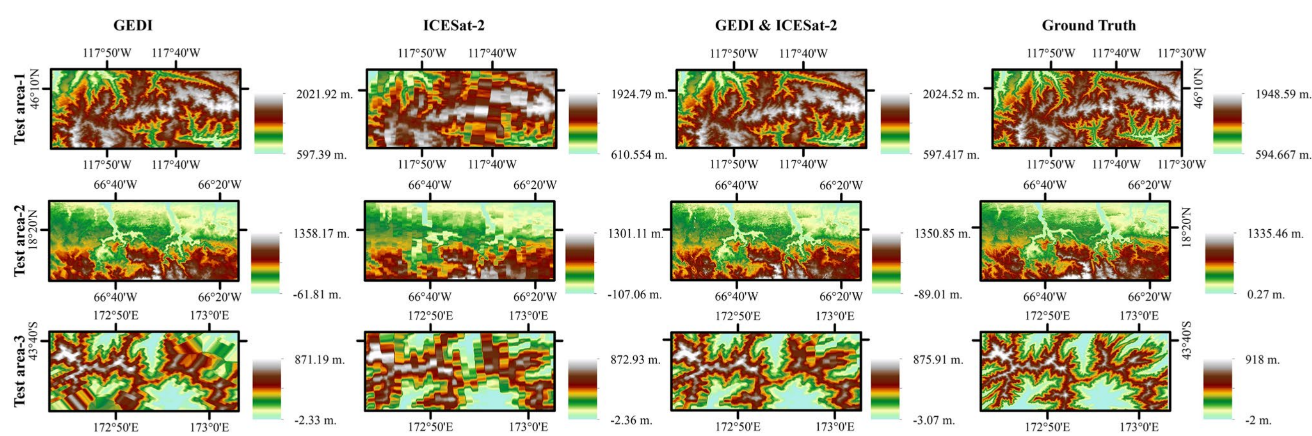

Fig. 6 DEMs produced by GEDI, ICESat-2 and GEDI & ICESat-2

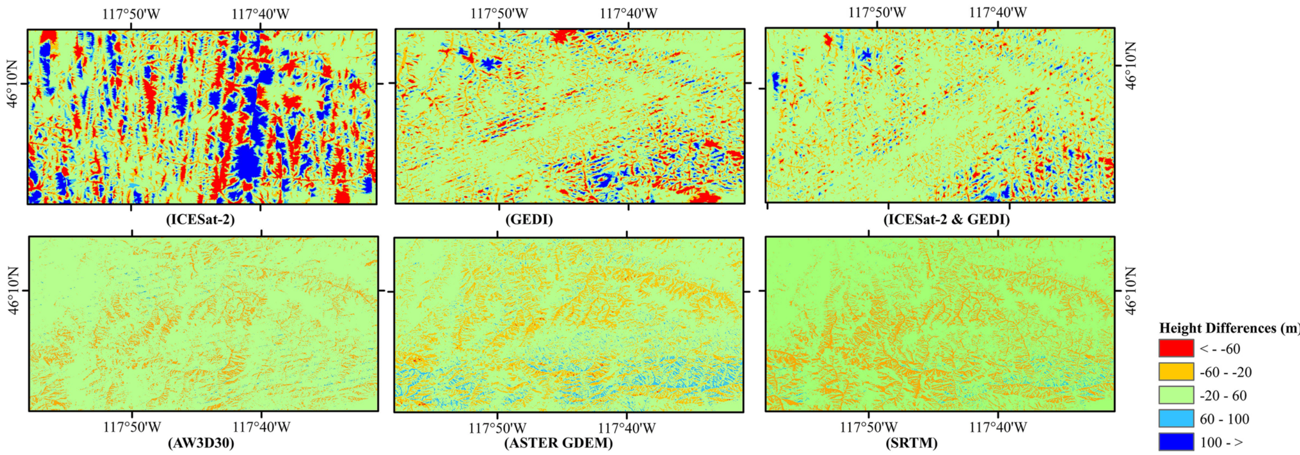

Fig. 7 Maps of height differences global DEMs and DEMs produced by GEDI, ICESat-2 in test area-1

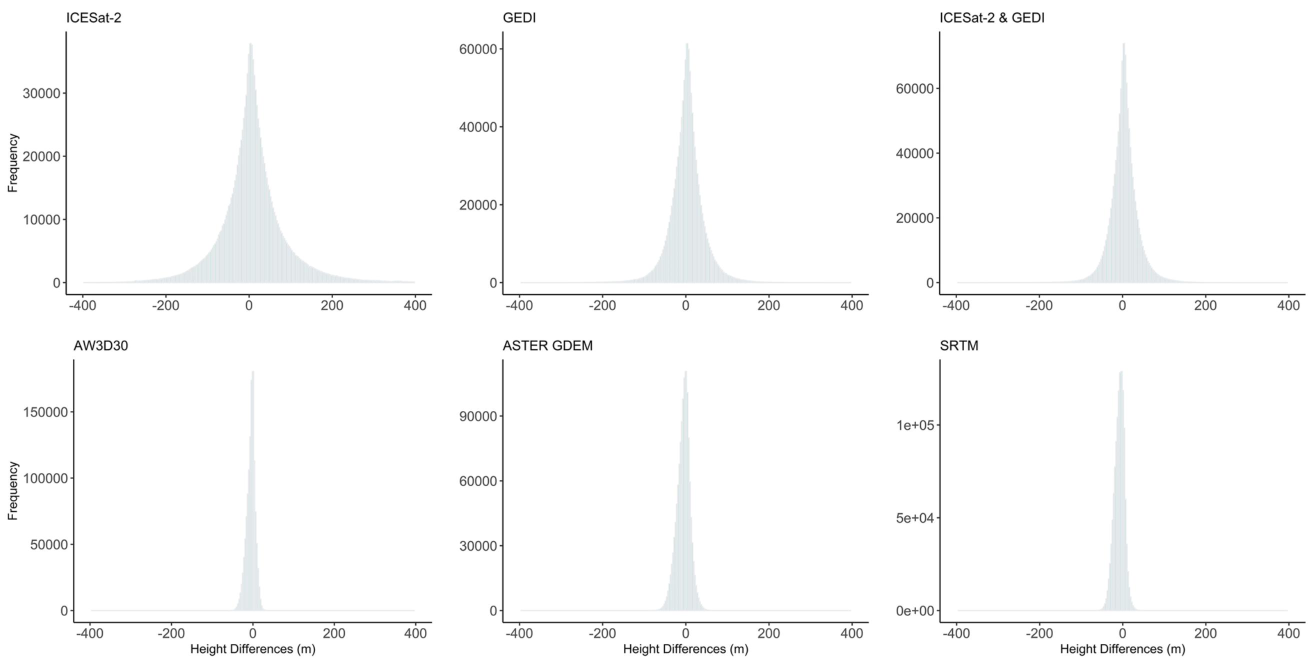

Fig. 8 Raster-based error histogram in test area-1

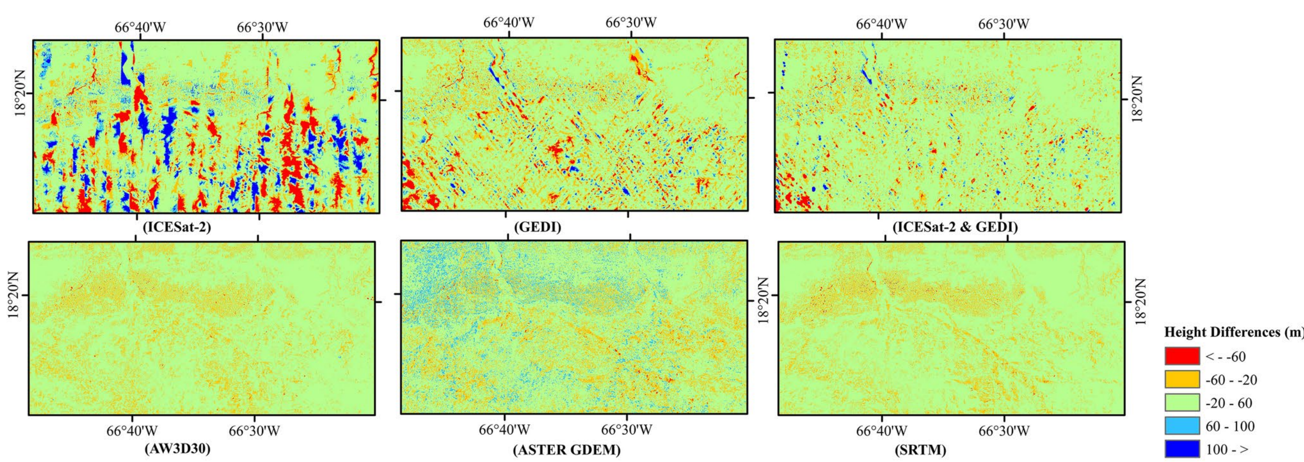

Fig. 9 Maps of height differences global DEMs and DEMs produced by GEDI, ICESat-2 in test area-2

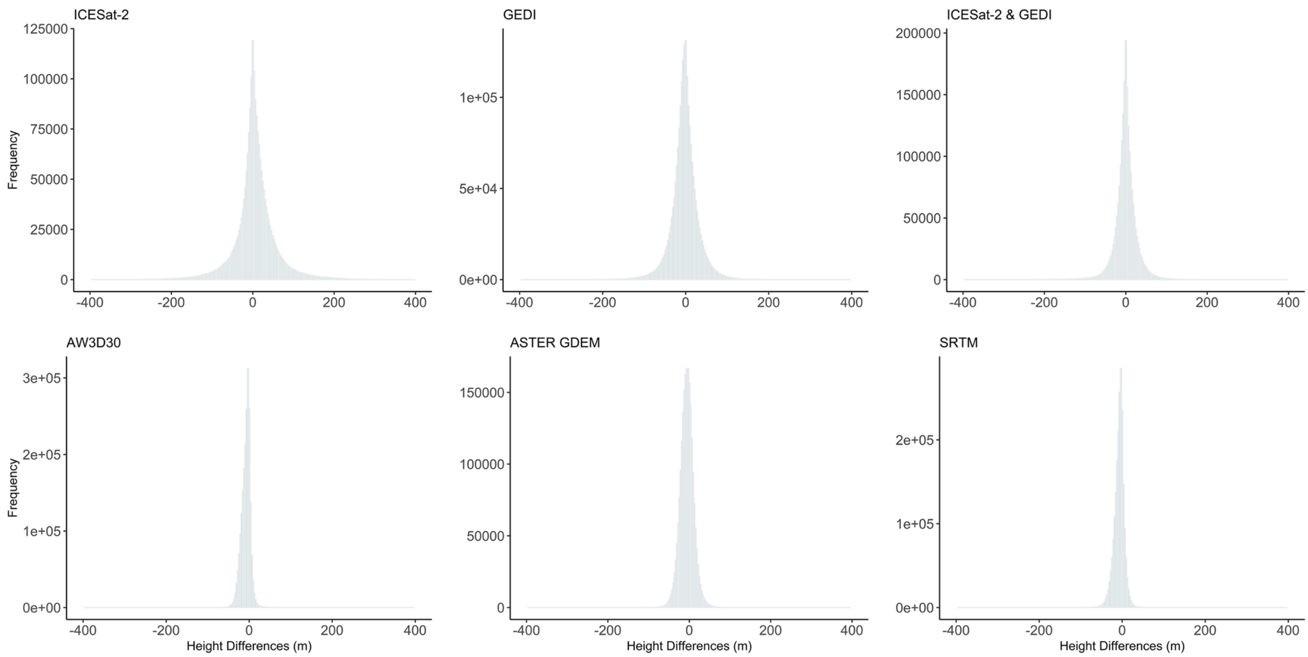

Fig. 10 Raster-based error histogram in test area-2

decreased from 1850 to 329 in one study area (Hanzhong area) and decreased from 1829 to 96 in the other region (Songshan Area). Although the vertical accuracy increases after filtering techniques are applied, the decrease in the number of points is a disadvantageous situation for DEM production. Especially in DEM production, the high number of points gives more consistent models since the reference point of the model will increase during interpolation. In our study, although ICESat-2 data gave better results than GEDI in point-based results, GEDI produced DEMs gave better results than ICESat-2 produced DEMs in raster-based results, compared to RMSE evaluation, excluding Test area-3. (Appendix Table 7). In Test Area-3, in areas where GEDI data density decreases (Fig. 1), it is seen that the DEM production results decreases according to the RMSE (Fig. 11). Test Area-3 GEDI data is close to the mission's coverage limits, so there has been a reduction in the number of points. This puts GEDI data at a disadvantage compared to ICESat-2 data. Because coverage of the ICESat-2 area is more than GEDI since it also includes poles. Considering the results of the study, it was revealed that DEMs produced by using two data together in all 3 fields gave more successful results compared to their individual results.

Also, considering the MAD results, it is seen that both point-based and raster-based results of SAS are good

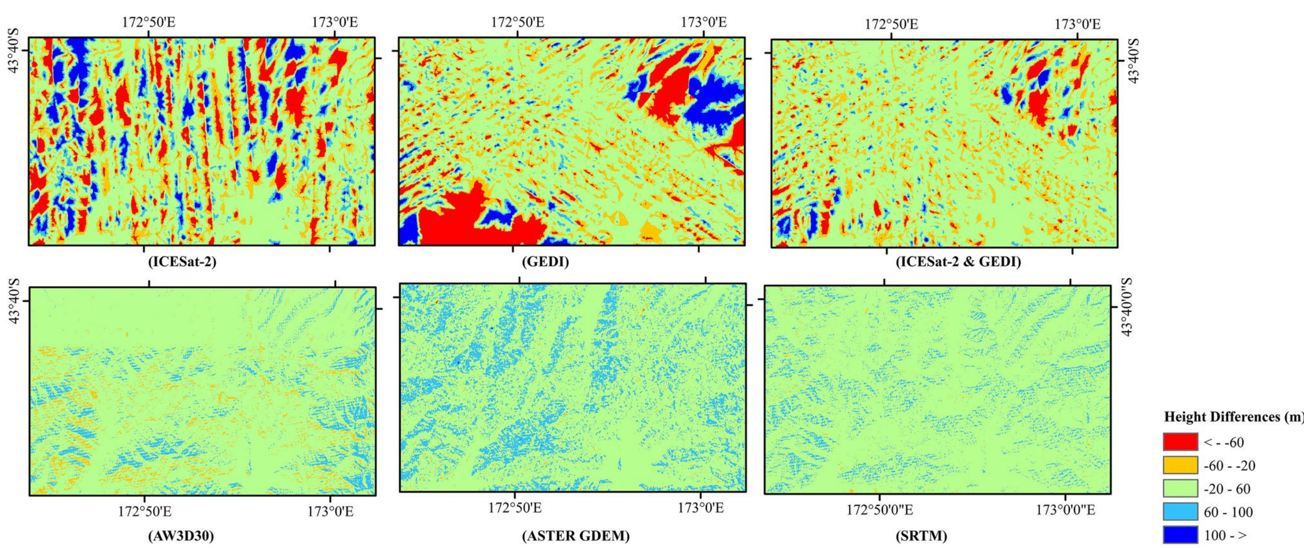

Fig. 11 Maps of height differences global DEMs and DEMs produced by GEDI, ICESat-2 in test area-3

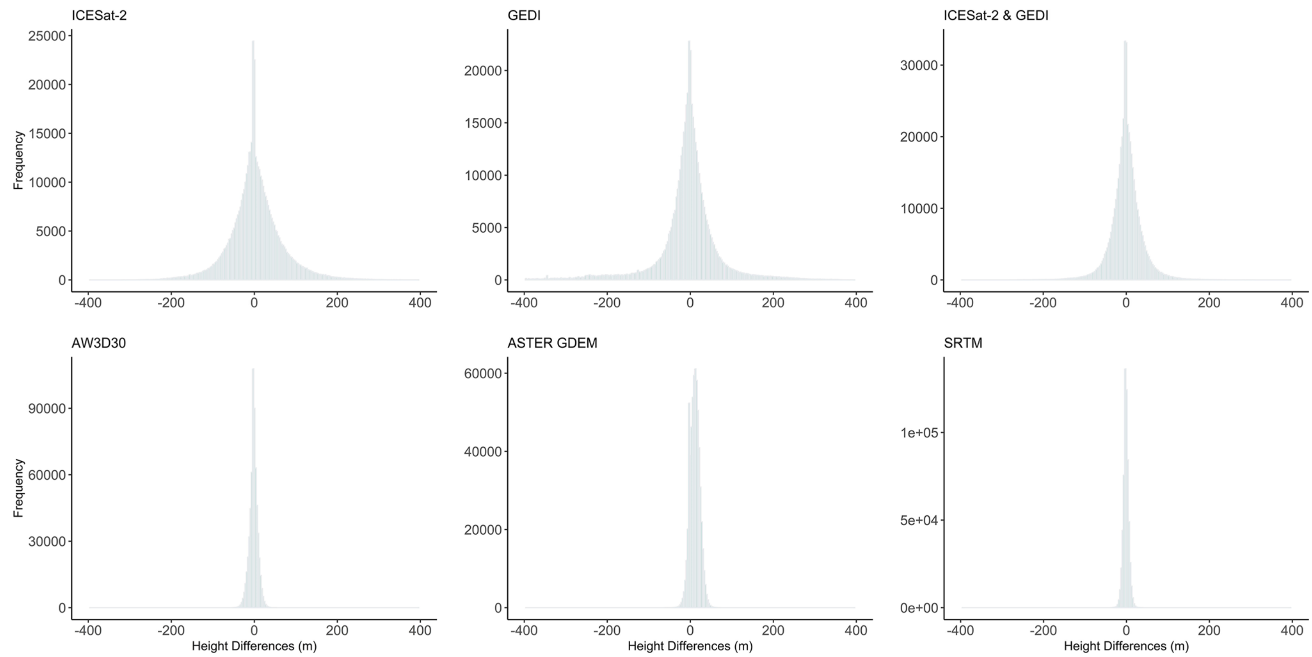

Fig. 12 Raster-based error histogram and boxplot plots in test area-3

according to GDEMs (Appendix Table 7). The reason for this is that MAD is a robust parameter calculated over the median, so it is less affected by the outlier. As a result of the increase in the number of points that ICESat-2 and GEDI satellites will collect until the end of their mission, better DEMs will be produced after outlier values are filtered out.

Conclusion

Different professional disciplines use the information obtained from DEM. For this reason, the production methods of DEMs differ. In our study, we focused on GDEMs and DEM producing from SAS. GDEMs are both outdated due to the years of production and contain systematic errors within themselves. For this reason, the accuracy of the satellite LiDAR data, which started collecting data at the end of 2018, was investigated both on a point based and its potential to create a DEMs. Considering the results of the study, it was seen that the ICESat-2 data in point-based results had similar accuracy with other GDEMs. In addition, DEMs produced by combining two data showed good results, indicating that better DEMs can be produced in the future with an increase in the number of points. However, it is less successful compared to today's free GDEMs because there are too many gaps. For this reason, it is considered to conduct studies on creating a new model with the fusion (like a NASADEM) of GDEMs and GEDI & ICESat-2 data using machine learning methods in future studies.

Fig. 13 Raster-based results based on ALS DEM data

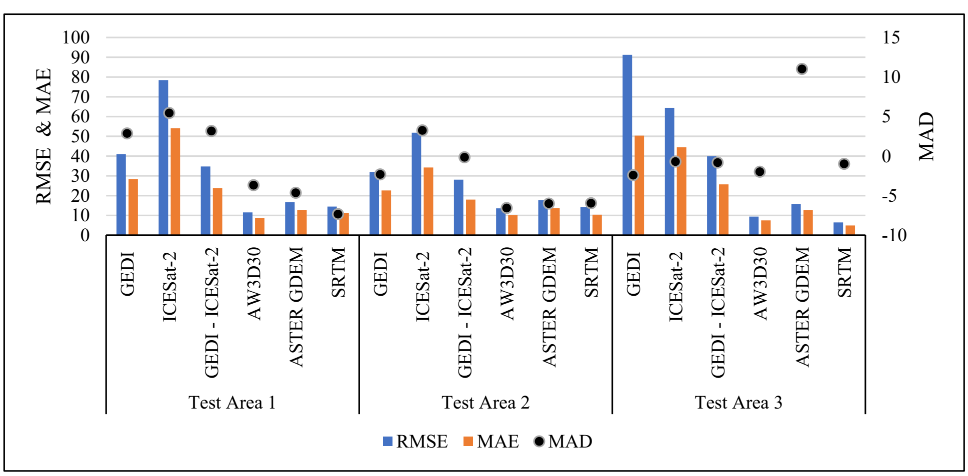

Appendix

Table 7 Result information of ground truth data. Light blue lines show point-based results, light green areas show raster-based results

		Correlation	RMSE	MAE	MAD
Test Area 1	GEDI	0.9961	22.350	17.021	3.530
	AW3D30	0.9991	12.292	16.227	6.065
	ASTER GDEM	0.9980	17.521	14.868	4.810
	SRTM	0.9989	15.235	13.350	7.888
	ICESat-2	0.9993	12.166	13.598	4.572
	AW3D30	0.9993	11.190	14.709	5.000
	ASTER GDEM	0.9985	16.291	13.668	3.510
	SRTM	0.9991	14.314	12.020	6.290
	GEDI DEM	0.9888	41.052	28.383	2.857
	ICESat-2 DEM	0.9589	78.430	54.145	5.429
	GEDI & ICESat-2 DEM	0.9921	34.740	23.857	3.156
	AW3D30	0.9993	11.543	8.741	3.700
	ASTER GDEM	0.9984	16.717	12.830	4.657
	SRTM	0.9991	14.435	11.291	7.347
Test Area 2	GEDI	0.9960	20.359	9.985	0.686
	AW3D30	0.9989	13.578	10.203	6.665
	ASTER GDEM	0.9972	17.995	13.967	6.682
	SRTM	0.9986	14.210	10.525	5.959
	ICESat-2	0.9960	13.746	7.135	2.050
	AW3D30	0.9989	13.052	9.700	5.989
	ASTER GDEM	0.9972	17.044	13.168	5.460
	SRTM	0.9986	13.546	10.021	5.639
	GEDI DEM	0.9891	31.998	22.618	2.333
	ICESat-2 DEM	0.9738	51.788	34.215	3.236
	GEDI & ICESat-2 DEM	0.9943	28.096	18.025	0.166
	AW3D30	0.9725	13.538	10.080	6.578
	ASTER GDEM	0.9980	17.759	13.606	6.021
	SRTM	0.9983	14.178	10.369	5.982
Test Area 3	GEDI	0.9981	11.952	8.511	0.226
	AW3D30	0.9989	9.442	5.060	1.000
	ASTER GDEM	0.9982	16.382	13.391	11.000
	SRTM	0.9994	6.623	7.007	2.000
	ICESat-2	0.9992	7.846	5.021	0.787
	AW3D30	0.9989	9.102	4.643	1.000
	ASTER GDEM	0.9984	15.614	12.555	11.000
	SRTM	0.9995	6.172	6.630	2.000
	GEDI DEM	0.8935	91.217	50.336	2.430
	ICESat-2 DEM	0.9473	64.391	44.479	0.717
	GEDI & ICESat-2 DEM	0.9800	39.954	25.707	0.843
	AW3D30	0.9989	9.398	7.445	2.000
	ASTER GDEM	0.9984	15.783	12.711	11.000
	SRTM	0.9995	6.434	4.884	1.000

Acknowledgements The study consists of the Ph.D. thesis of the first author.

Author contributions The authors have equal contributions.

Funding This research was supported by the Afyon Kocatepe University (Project Number: 22.FEN.BİL.02).

Data availability statement The datasets generated during and/or analysed during the current study are available from the corresponding author on reasonable request.

Declarations

Conflict of interest The authors declare no conflict of interest.

References

Abdallah A, Saifeldin A, Abomariam A, Reda A (2020) Efficiency of using GNSS-PPP for digital elevation model (DEM) production. Artific Sat 55(1):17–28

Adam M, Urbazaev M, Dubois C, Schmullius C (2020) Accuracy assessment of GEDI terrain elevation and canopy height estimates in European temperate forests: Influence of environmental and acquisition parameters. Remote Sens 12(23):3948

Banjo OB, Salami WA, Adewale RO, Adegoke A (2021) Spot height digital elevation model of Yewa division, Ogun State Nigeria. Fed Univ Wukari Trends Sci Technol J 6(2):436–440

Burrough PA (1986) Principles of geographical. Information systems for land resource assessment. Clarendon, Oxford

Dubayah R, Blair JB, Goetz S, Fatoyinbo L, Hansen M, Healey S, … Silva C (2020) The Global Ecosystem Dynamics Investigation: High-resolution laser ranging of the Earth's forests and topography. Sci Remote Sens 1:100002

El Mhamdi A, Aarab M, El Fariati A (2023) Evaluation of the Accuracy of Open-Source DEMs using GPS Data. Int J Environ Geoinform 10(1):41–50

Erdogan S (2009) A comparision of interpolation methods for producing digital elevation models at the field scale. Earth Surf Proc Land 34(3):366–376

Fayad I, Baghdadi N, Bailly JS, Frappart F, Zribi M (2020) Analysis of GEDI elevation data accuracy for inland waterbodies altimetry. Remote Sensing 12(17):2714

Heritage GL, Milan DJ, Large AR, Fuller IC (2009) Influence of survey strategy and interpolation model on DEM quality. Geomorphology 112(3–4):334–344

Ince ES, Barthelmes F, Reißland S, Elger K, Förste C, Flechtner F, Schuh H (2019) ICGEM–15 years of successful collection and distribution of global gravitational models, associated services, and future plans. Earth Syst Sci Data 11(2):647–674

Jaber WA, Floricioiu D, Rott H, Eineder M (2013) Surface elevation changes of glaciers derived from SRTM and TanDEM-X DEM differences. 2013 IEEE International Geoscience and Remote Sensing Symposium - IGARSS, Melbourne, VIC, Australia, pp. 1893–1896. https://doi.org/10.1109/IGARSS.2013.6723173

Kassim AR, Misman MA, Faidi MA, Omar H (2016) A tool for assessing ecological status of forest ecosystem. IOP Conf Ser Earth Environ Sci 2016(37). https://doi.org/10.1088/1755-1315/37/1/012026

Khalsa SJS, Borsa A, Nandigam V, Phan M, Lin K, Crosby C, … Lopez L (2020) OpenAltimetry-rapid analysis and visualization of Spaceborne altimeter data. Earth Sci Inform 1–10. https://doi.org/10.1007/s12145-020-00520-2

Kokalj Ž, Mast J (2021) Space lidar for archaeology? Reanalyzing GEDI data for detection of ancient Maya buildings. J Archaeol Sci Rep 36:102811

Lemoine FG, Kenyon SC, Factor JK, Trimmer RG, Pavlis NK, Chinn DS, ... Olson TR (1998) The development of the joint NASA GSFC and the National Imagery and Mapping Agency (NIMA) geopotential model EGM96 (No. NAS 1.60: 206861)

Liu X, Zhang Z, Peterson J, Chandra S (2008) Large area DEM generation using airborne LiDAR data and quality control. In: Accuracy in Geomatics: Proceedings of the 8th International Symposium on Spatial Accuracy Assessment in Natural Resources and Environmental Sciences, v. 2, vol. 2, pp. 79–85

Liu A, Cheng X, Chen Z (2021) Performance evaluation of GEDI and ICESat-2 laser altimeter data for terrain and canopy height retrievals. Remote Sens Environ 264:112571

Mesa-Mingorance JL, Ariza-López FJ (2020) Accuracy assessment of digital elevation models (DEMs): A critical review of practices of the past three decades. Remote Sensing 12(16):2630

Milan DJ, Heritage GL, Large AR, Fuller IC (2011) Filtering spatial error from DEMs: Implications for morphological change estimation. Geomorphology 125(1):160–171

Muslim AM, Foody GM (2008) DEM and bathymetry estimation for mapping a tide-coordinated shoreline from fine spatial resolution satellite sensor imagery. Int J Remote Sens 29(15):4515–4536

Neuenschwander AL, Magruder LA (2019) Canopy and terrain height retrievals with ICESat-2: A first look. Remote Sensing 11(14):1721

Neuenschwander AL, Pitts KL, Jelley BP, Robbins J, Klotz B, Popescu SC, Nelson RF, Harding D, Pederson D, Sheridan R (2020) ATLAS/ICESat-2 L3A Land and vegetation height, version 3. [Test areas]. Boulder, Colorado USA. NASA National Snow and Ice Data Center Distributed Active Archive Center. https://doi.org/10.5067/ATLAS/ATL08.003

Oliver MA, Webster R (1990) Kriging: a method of interpolation for geographical information systems. Int J Geogr Inform Syst 4(3):313–332

Park SJ, McSweeney K, Lowery B (2001) Identification of the spatial distribution of soils using a process-based terrain characterization. Geoderma 103(3–4):249–272

Petrasova A, Mitasova H, Petras V, Jeziorska J (2017) Fusion of high-resolution DEMs for water flow modeling. Open Geospatial Data, Software Standards 2(1):1–8

Preety K, Prasad AK, Varma AK, El-Askary H (2022) Accuracy assessment, comparative performance, and enhancement of public domain digital elevation models (aster 30 m, srtm 30 m, cartosat 30 m, srtm 90 m, merit 90 m, and tandem-x 90 m) using DGPS. Remote Sens 14(6):1334

Quirós E, Polo ME, Fragoso-Campón L (2021) GEDI Elevation Accuracy Assessment: A Case Study of Southwest Spain. IEEE J Select Topics Appl Earth Observ Remote Sens 14:5285–5299

Santillan JR, Makinano-Santillan M (2016) Vertical accuracy assessment of 30-M resolution ALOS, ASTER, and SRTM global DEMS over Northeastern Mindanao, Philippines. Int Arch Photogramm Remote Sens Spat Inf Sci 41:149–156. https://doi.org/10.5194/isprs-archives-XLI-B4-149-2016

Setiyoko A, Kumar A (2012) Comparison analysis of interpolation techniques for DEM generation using Cartosat-1 stereo data. Int J Remote Sens Earth Sci (IJReSES) 9(2):78–87. https://doi.org/10.30536/j.ijreses.2012.v9.a1829

Shang D, Zhang Y, Dai C, Ma Q, Wang Z (2022) Extraction Strategy for ICESat-2 Elevation Control Points Based on ATL08 Product. IEEE Trans Geosci Remote Sens 60:1–12

Sunila R, Kollo K (2007) A comparison of geostatistics and fuzzy application for digital elevation model. Int Arch Photogramm Remote Sens Spat Inf Sci 34. http://www.isprs.org/proceedings/XXXVI/2-C43/Session2/paper_Sunila_Kollo.pdf

Team RC (2013) R: A language and environment for statistical computing. (R Foundation for Statistical Computing) https://www.r-project.org/

Urbazaev M, Hess LL, Hancock S, Sato LY, Ometto JP, Thiel C, …, Schmullius C (2022) Assessment of terrain elevation estimates from ICESat-2 and GEDI spaceborne LiDAR missions across different land cover and forest types. Sci Remote Sens 6:100067

Uysal M, Toprak AS, Polat N (2015) DEM generation with UAV Photogrammetry and accuracy analysis in Sahitler hill. Measurement 73:539–543

Wong WV, Tsuyuki S, Ioki K, Phua MH (2014) Accuracy assessment of global topographic data (SRTM & ASTER GDEM) in comparison with LIDAR for tropical montane forest. In: Proceedings of the 35th Asian Conference on Remote Sensing, Nay Pyi Taw, Myanmar, 27–31 October 2014, pp. 722–727

Yap L, Kandé LH, Nouayou R, Kamguia J, Ngouh NA, Makuate MB (2019) Vertical accuracy evaluation of freely available latest high-resolution (30 m) global digital elevation models over Cameroon (Central Africa) with GPS/leveling ground control points. Int J Digital Earth 12(5):500–524